

Fetal Heart Rate Complexity Measures to Detect Hypoxia

Óscar Barquero-Pérez, Rebeca Goya-Esteban, Antonio Caamaño, Carlos Martín-Caballero and José Luis Rojo-Álvarez

Abstract

Background Perinatal hypoxia is a severe condition that may harm fetus organs permanently or even cause dead. When the fetus brain is partially deprived from oxygen, the control of the fetal heart rate (FHR) is affected.

Objective. We hypothesize that the complex physiological mechanisms of the FHR are perturbed under perinatal hypoxia. We propose measure entropy and time irreversibility of the FHR to quantify the loss in the complexity.

Materials and Methods. We estimated the complexity of the FHR signal using Sample Entropy (SampEn), Permutation Entropy (PE), and Time Irreversibility (TI). We compared the results with time (Short Time Variability, STV) and frequency domain (High Frequency Power, PHF) methods. We computed every one hour before delivery. FHR traces were preprocessed to remove artifacts. A database of 32 FHR recordings were acquired with cardiotocography, 15 controls and 16 cases. A case was declared whether: 1) the PH of the umbilical artery was ≤ 7.05 ; or 2) the APGAR score 5 minutes after delivery was ≤ 7 and a reanimation type III or greater was required. Resampling methods were used to establish the statistical differences.

Results. TI was significantly different for healthy and hypoxia fetuses (-0.38 ± 0.19 vs. -0.21 ± 0.37 , $p\text{-value}=0.063$). Entropy indices were higher for healthy fetuses (SampEn: 0.33 ± 0.12 vs 0.28 ± 0.09 , $p\text{-value}=0.11$; PE: 0.72 ± 0.04 vs 0.69 ± 0.07 , $p\text{-value}=0.12$). STV (3.23 ± 1.15 vs 3.45 ± 1.35 , $p\text{-value}=0.30$) and PHF (0.40 ± 0.18 vs 0.43 ± 0.25 , $p\text{-value}=0.31$) indices showed no differences.

Conclusions. Complexity measures of the FHR were different for healthy and hypoxia fetuses. These indices may help to early detect hypoxia with less invasive methods.

1. Introduction

2. Methods

The proposed system consists of several stages, namely: time series segmentation and feature extraction from FHR signals; similarity calculation with NCD, for which the

combination of similarity matrices can provide with further advantage; and choice of a suitable classification algorithm for the final purpose of hypoxia detection. The theoretical basis and design criteria of these stages are described below.

2.1. Permutation Entropy

Here your code

2.2. Time Irreversibility

Here your code

2.3. Test Hypothesis Bootstrap

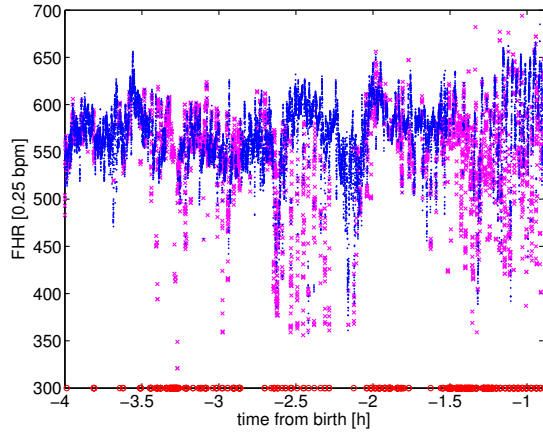
Here your code

3. Data description

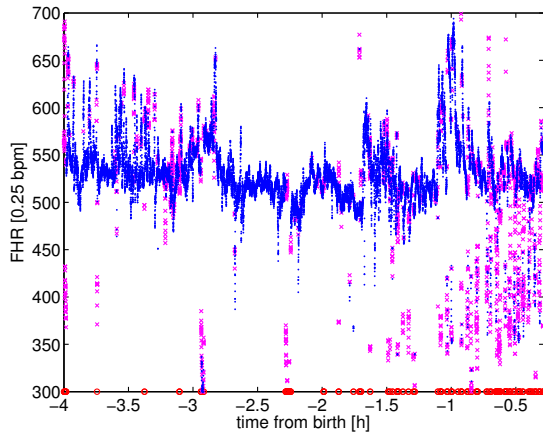
FHR records¹ were acquired with a Philips cardiotocograph for a total of 32 recordings, 15 controls and 17 cases. A case was declared whether: 1) the PH of the umbilical artery was ≤ 7.05 ; or 2) the APGAR score was ≤ 7 at 5 minutes after delivery and a reanimation type III or greater was required. The institutional Medical Ethics Review Board approved the use of this data.

Records, see Figure 1 for an example, have considerable variability both in start/ending times and pauses as labor duration vary. In addition, the cardiotocograph may be disconnected at any time for a number of reasons. Also, the signal is lost sometimes as the fetus and mother move. The cardiotocograph provides three signal qualities (lost, medium and high). We decided to consider the window between 4 to 1 hours before birth for our analysis, even though not all patients have signal along all this window, e.g. nine patients even start being monitored after 4 hours to delivery (8 cases) or they are removed the cardiotocograph before 1 hour to delivery (one case). When a patient has no signal in the entire interval analyzed in a experiment, it was excluded (see below).

¹Data is available from the website: <http://sites.google.com/site/hufahypoxia>.



(a) hypoxic



(b) control

Figure 1. FHR for (a) a hypoxic and (b) a control patient. Signal qualities are 9.9% lost, 19.2% medium and 70.9% high for (a) ; and 1.8% lost, 9.8% medium and 88.3% high for (b). Signal qualities high, medium and lost are respectively represented by the markers: “ \cdot ”, “ \times ” and “ \circ ”.

4. Results

The experimental results are presented by following the next sequence:

- We started by evaluating the classification performance in FHR records, without any preprocessing, using only the NCD similarity criterion and a nearest neighbor classifier. This experiment evaluated the performance of NCD and set the baseline accuracy that could be attained.
- Next, we considered as features for hypoxia classification the aforementioned time and frequency indices that are commonly used in HRV analysis, aiming to evaluate whether they showed some improvement over NCD raw analysis.

- Then, we analyzed the performance obtained by using as features the general purpose statistical moments applied to the raw signals.
- We also performed feature selection on each group of variables (time and frequency HRV indices and statistical moments), in order to identify the best features and to see whether feature selection could improve classification performance.
- The experiments continued by evaluating whether the NCD could empower the HRV parameters and statistical moments by obtaining the similarity of the (possibly different length) sequences that result of their application on sliding windows.

4.1. Raw data analysis

In this experiment, we analyzed the FHR raw signals in the four time intervals described before. We analyzed three types of signals: a) including only high quality signals; b) including also medium quality signals; c) including also medium quality and lost (represented with zeros) signals.

By using NCD, a dissimilarity matrix was created with all pairwise dissimilarities among signals. We used the software provided by NCD authors [1] to compute the NCD for the signals with three compressor types (zip, bzip2, and lzma). The accuracy was estimated by using LOO cross-validation with a nearest neighbour classifier.

Best results are summarized in Table 1, where we can see that high quality signal and the interval from 4 to 3 hours before delivery are the best for prediction accuracy (0.73). In addition, we see that, for the same time interval, the prediction using all the signal is better than using only high and medium qualities, which shows that taking into account lost signals that may occur when the fetus moves, might increase prediction accuracy. Best prediction accuracy for all the patients (4 to 1 hours to delivery interval) was done again considering only high quality signal, but it did not rise above 0.66.

4.2. Time and frequency HRV indices

We obtained a set of relevant time HRV descriptors for the considered time intervals. We used all signal qualities, but in this experiment, interpolation was performed on the beats classified as artifacts, as described in Section ???. Then, we standardized (zero-mean, unit-variance) each descriptor and combined all of them in a vector. We benchmarked the following classifiers: nearest neighbour (NN), k nearest neighbours (k -NN), and SVM with linear (SVC) and radial basis function (RBF-SVC) kernels. As these features were not designed as dissimilarities, we tried also the SVM, both to compare its performance with nearest neighbour based classifiers, and to try to extract the best performance of these indices. Table 2 shows the results

Table 1. NCD and nearest neighbor classifier best results for raw signals. “Quality” shows the types of signal included in the analysis (High,Medium,Low). “Interval” expresses the signal interval in hours to delivery. “T/C” shows the number of conTrols and Cases, respectively. “Acc.”, “Sen.” and “Spe.” stand for accuracy, sensitivity and specificity, respectively; and “Sym.” shows the method used to make the dissimilarity matrix symmetric.

Quality	T/C	Interval	Acc.	Sen.	Spe.	Compressor	Sym.
H	13/13	4 ↔ 3	0.73	0.69	0.77	zip	min
H	13/14	3 ↔ 2	0.63	0.57	0.69	bzip2	min
H	15/16	2 ↔ 1	0.58	0.75	0.40	lzma	mean
H	15/17	4 ↔ 1	0.66	0.82	0.47	zip	min
HM	13/13	4 ↔ 3	0.58	0.62	0.54	zip	min
HM	13/14	3 ↔ 2	0.56	0.79	0.31	bzip2	min
HM	15/16	2 ↔ 1	0.55	1.0	0.07	lzma	mean
HM	15/17	4 ↔ 1	0.56	0.59	0.53	lzma	min
HML	13/13	4 ↔ 3	0.66	0.77	0.54	zip	min
HML	13/14	3 ↔ 2	0.56	0.14	1.0	lzma	min
HML	15/17	2 ↔ 1	0.53	0.76	0.27	lzma	min
HML	15/17	4 ↔ 1	0.59	0.59	0.60	zip	min

of leave one out cross-validation. The best performance (0.74 accuracy) was obtained in the 3 ↔ 2 interval by a SVM classifier.

We repeated the same experiments with the commonly used frequency HRV indices considered above. Results are shown in Table 2. Again, the best results (0.74 accuracy) were obtained in the 3 ↔ 2 interval by k-NN. The combination of the Time and Frequency indices (table not shown) gave a maximum accuracy of 0.70 in the 3 ↔ 2 interval with all classifiers but 1-NN. The best results obtained by these methods provided almost no gain over raw analysis.

4.3. Statistical Moments

In order to compute the moments on the records including high and medium signal qualities, we firstly scaled the FHR signal dividing it by the maximum value of each moment for all patients. Then, we calculated raw and central moments of orders $n = \{1, 2, \dots, 10\}$ for each patient. Finally, the moments were applied the transformation $x \rightarrow \sqrt[k]{x}$, where k is the order of the moment, and standardized (zero-mean and unit-variance). The results of classifying the records with these moments are also shown in Table 2, where a 0.69 accuracy was obtained in the 4 to 3 hours and in the 4 to 1 hours before delivery intervals. Again, no real gain was obtained by these set of features over the raw analysis.

4.4. Feature Selection

Sometimes, the learning task can be simplified and even improved by selecting variables. In this section, we applied forward selection (FS) to HRV (time and frequency)

Table 2. HRV time and frequency indices and statistical moments accuracy for the considered time intervals. SVC and RBF-SVC stand for linear and radial basis kernel Support Vector Classifier, respectively.

Interval	Features	1-NN	k-NN	SVC	RBF-SVC
4 ↔ 3	Time	0.69	0.69	0.35	0.5
3 ↔ 2		0.70	0.67	0.74	0.74
2 ↔ 1		0.59	0.5	0.47	0.47
4 ↔ 1		0.47	0.5	0.5	0.37
4 ↔ 3	Frequency	0.54	0.65	0.62	0.46
3 ↔ 2		0.56	0.74	0.67	0.70
2 ↔ 1		0.58	0.58	0.42	0.23
4 ↔ 1		0.5	0.5	0.53	0.44
4 ↔ 3	Moments	0.69	0.62	0.46	0.58
3 ↔ 2		0.22	0.63	0.59	0.52
2 ↔ 1		0.23	0.065	0.48	0.29
4 ↔ 1		0.5	0.44	0.69	0.59

indices and to statistical moments. The results of applying FS to the time HRV indices, shown in Table 3, were in general not better than the obtained without feature selection, as maximum overall accuracy decreased to 0.72, which was found in the interval 2 to 1 hours to delivery, where, however, it improved the previous (0.59) result. FS algorithm consistently selected *stdFHR* as the unique feature for classification for this case.

The results for FS on the frequency HRV indices, shown in Table 3, were slightly better than without feature selection. FS slightly improved the result in all time intervals. The best result (0.75 accuracy) was attained on the 4 to 1 hours to delivery interval. FS algorithm consistently selected $P_{LF}/(P_{MF} + P_{HF})$ as the single classification feature for this case.

The results of FS on the statistical moments improved the maximum accuracy obtained in Table 2 with a moderate increase (from 0.69 to 0.73). Most selected features for the interval 4 to 3 hours to delivery, where the highest accuracy was attained (0.73), were μ_4 , μ_8 , and μ_9 .

4.5. Time and Frequency Indices in Sliding Windows

A HRV parameter or a statistical moment provides us with a single value for a signal. If we divide the signal in equal sized windows we got more values, but when comparing these values with the ones from another patient, both signals should have same length, which will not happen in practice. On the other hand, it is easy to obtain a similarity on signals or sequences of different lengths by using NCD. Therefore, the use of NCD allows us to compare signals from two patients by using the fine grained description provided by the time evolution of a given statis-

Table 3. Forward selection accuracy in HRV time and frequency indices and statistical moments for the considered time intervals.

Interval	Features	1-NN	k-NN	SVC	RBF-SVC
4 ↔ 3	Time	0.54	0.54	0.27	0.35
3 ↔ 2		0.48	0.67	0.63	0.59
2 ↔ 1		0.72	0.72	0.44	0.69
4 ↔ 1	Frequency	0.34	0.34	0.56	0.38
4 ↔ 3		0.62	0.62	0.077	0.65
3 ↔ 2		0.52	0.59	0.74	0.67
2 ↔ 1		0.65	0.48	0.19	0.55
4 ↔ 1	Moments	0.75	0.75	0.34	0.41
5 4 ↔ 3		0.73	0.73	0.19	0.69
3 ↔ 2		0.26	0.3	0.41	0.3
2 ↔ 1		0.42	0.39	0.42	0.42
4 ↔ 1		0.41	0.34	0.44	0.41

tic obtained in a sliding window. Note that this approach also evaluates whether a sequence obtained by sequentially calculating a statistic in a sliding window could have information that can be better exploited by the compressor than the raw signal, which would be (not possible in theory if the perfect Kolmogorov Complexity could be calculated, but it would be possible in practice as compressors are not perfect. Therefore, we considered the calculation of new signals from obtaining these statistics in each time interval of FHR analysis, and we evaluated the performance of obtaining the similarities of these signals for all patients with NCD and by classifying the result with a nearest-neighbour classifier.

For each time interval, we used the NCD to analyze the time and frequency indices in 5-minute sliding windows, where a window is only considered if its data had not too many artifacts (see Section ??). For each parameter, a sequence was constructed for each patient by concatenating the parameter value for each sliding window of the FHR signal. An NCD matrix for each parameter was later constructed by obtaining the similarities among all pairs of patient sequences, and the accuracy of a nearest neighbour classifier was estimated by leave-one-out cross-validation.

Table 4 shows the best individual accuracies of the HRV time indices in each analysis interval. The best result (0.70 accuracy, 0.86 sensitivity and 0.54 specificity) was again in the 3 ↔ 2 interval by using the LTI index. We combined the 4 time indices by voting, and the best result gave an accuracy of 0.66 with sensitivity of 0.76 and specificity of 0.53 in the 4 ↔ 1 interval, which was better than the result provided by adding the dissimilarity matrices.

Table 4 also shows the best individual accuracies of the HRV frequency indices. The best result (0.77 accuracy, 0.77 sensitivity and 0.77 specificity) was in the 4 ↔ 3 interval by using $P_{LF}/(P_{MF} + P_{HF})$. Different indices seemed to be the most informative in each interval. We

Table 4. NCD and nearest neighbour classifier best results for HRV time and frequency indices and statistical moments in 5-minute sliding-windows signals.

Interval	Features	Acc.	Sen.	Spe.	Feature	Comp.	Sy.
4 ↔ 3	Time	0.62	0.69	0.54	$sdFHR$	bzip2	n
3 ↔ 2		0.70	0.86	0.54	LTI	lzma	n
2 ↔ 1		0.66	0.65	0.67	\overline{FHR}	bzip2	n
4 ↔ 1	Frequency	0.69	0.76	0.6	\overline{FHR}	bzip2	n
4 ↔ 3		0.77	0.77	0.77	$\frac{P_{LF}}{P_{MF} + P_{HF}}$	bzip2	n
3 ↔ 2		0.59	0.64	0.54	P_{VLF}	bzip2	n
2 ↔ 1		0.69	0.65	0.73	P_{HF}	bzip2	n
4 ↔ 1	Moments	0.69	0.88	0.47	P_{LF}	lzma	m
4 ↔ 3		0.88	0.92	0.85	μ_3	lzma	n
3 ↔ 2		0.70	0.64	0.77	μ_2	bzip2	n
2 ↔ 1		0.77	0.81	0.73	M_4	zip	m
4 ↔ 1		0.81	0.82	0.80	M_4	lzma	m

combined the 6 frequency indices by adding the dissimilarity matrices, and the best result gave an accuracy of 0.69 with sensitivity of 0.53 and specificity of 0.85 in the 4 ↔ 3 interval.

4.6. Moments in Sliding Windows

In this experiment, we used high and medium signal qualities and 5 minutes sliding windows. For each window, we computed raw and central moments of orders $n \in \{1, 2, \dots, 10\}$. Then, for each moment of order n , the results of all windows were concatenated to obtain the new signal $s_{i,n}$ that provided a description of the patient i . Later, this signal was transformed as $\bar{s}_{i,n} = \sqrt[n]{s_{i,n}}/A_n$ where A_n is the maximum value of the signals $\{s_{i,n}\}_{i=1}^{N_T}$. Then, the NCD pairwise distances were obtained for pairs $(\bar{s}_{i,n}, \bar{s}_{j,n})$ and accuracies were estimated using leave-one-out cross-validation with a nearest neighbour classifier.

The results are summarized in Table 4. The best predictive interval was the 4 to 3 hours to delivery. The best accuracy for individual moments gave an accuracy of 0.88 (23 out of 26), a sensitivity of 0.92 (12 out of 13) and a specificity of 0.85 (11 out of 13). In addition, we noted the good performance of the 4 to 1 hours to delivery interval, which can be applied to any record of our database, 0.81 accuracy (26 out of 32), 0.82 sensitivity (14 out of 17) and 0.80 specificity (12 out of 15).

5. Discussion and Conclusions

Several indices have been proposed to analyze FHR. The most common indices are based on time domain and frequency domain methods [2, 3]. Time domain methods aim to assess the long and short term variability of the FHR, whereas frequency domain methods aim to charac-

terize the oscillatory contributions on the FHR. In many cases these indices are reduced to a single number obtained in the entire time series or to a collection of numbers obtained in 5-minute windows slides, which are again reduced to a few numbers like mean or standard deviation.

We have proposed NCD as a similarity measure for FHR registers because it is able to exploit both linear and non-linear relations among records. We tried it with raw FHR records, time and frequency indices and moments signals extracted from sliding windows. We obtained better performance from the moments than from the raw records, which shows that the compressor is not able to extract all the relations in the data and preprocessing might help. Then, we have shown how to combine several moments (or other type of variable) by using a simple voting scheme and by summing the dissimilarity matrices, which provide overall better results in our case.

Main strengths of using NCD for comparing FHR registers or signals of any statistic applied to signal windows are simplicity and generality. Other commonly used information-theoretical measures, like Approximate entropy [4] or Sample entropy [5], need to tune the embedding dimension and specially the tolerance, which is a continuous parameter; but there is no parameter to tune for our approach. Indeed, despite we have tried three compressors and two simple approaches to get a symmetric matrix the proposed methodology can be straightforwardly used with a lzma compressor and the min approach to get symmetric NCD matrices. In addition, there is no problem with the common signal losses, which is a problem to apply frequency-related methods as they need signal interpolation, which is not always possible. The similarity can always be computed independently of how the signal losses are addressed.

Visual interpretation values basal FHR, its accelerations and decelerations in relation to uterine contractions, and beat-to-beat FHR variability [6, 7]. The following signal types are considered clearly pathological (suspicious of hypoxia): late decelerations, whose nadir has a delay of at least 30 seconds with respect to the acme of contractions; maintained bradycardia; low variability (less than 5 beats); and a “sine”-rhythm, named after its wave-like appearance, which is characterized by a long-term variability but almost no variability in the short-term.

First, late decelerations are produced in the following manner. During uterine contraction, when the myometrium pressure exceeds the blood pressure of the intervillous space of the placenta, maternal circulation is interrupted and therefore ceases to carry oxygen to the fetal territory. In a well oxygenated fetus, this is not a problem since the fetus does not consume all the tissue-oxygen before the end of the contraction. In a fetus with poor

oxygenation, on the other hand, the oxygen reserves are exhausted before the end of contraction and, particularly in the more sensitive heart cells (which act as a pacemaker), action-potential production mechanisms are delayed, which causes bradycardia.

And second, the decrease in variability is more difficult to explain. On the one hand, the regulation of FHR, usually controlled by the vagus nerve, is stopped by cardiac and nervous system hypoxia. On the other hand, it seems that there are less functionally active cells in the pacemaker as the hypoxia progresses. The regulatory system loses “degrees of freedom”, which therefore becomes increasingly uniform and deterministic [8].

FHR signal can be measured in two ways, namely, external, by using an ultrasonic sensor that observes the Doppler effect; and internal, in which fetal electrocardiogram (ECG) is measured with an electrode in the fetus scalp. Uterine activity can also be measured in two ways: by using a non-invasive pressure transducer in the mother’s abdomen, or with an invasive intrauterine catheter pressure sensor.

Automatic analysis of CTG has also been proposed. In [9], automatic ST analysis (the ST segment connects the QRS complex and the T wave) combined with CTG was shown to increase the ability of obstetricians to identify hypoxia and to improve the perinatal outcome. In [10], a clinical trial was proposed to assess whether computer analysis and alerts improves visual CTG monitoring. A system-identification approach was proposed [11] to model FHR and uterine activity as an input-output system, reporting around 50% sensitivity with 7.5% of false positives at 1h and 40 minutes before delivery. Time-frequency analysis and features from time-frequency space decomposition were successfully used in an animal study yielding 93% sensitivity and 98% specificity[12]. Other non-invasive approaches have been proposed to complement CTG, such as Doppler velocimetry and pulse oximetry [13–15], or near-infrared spectroscopy to measure cerebral metabolic rate of oxygen [16]. The performance of automatic approaches currently applied to hypoxia detection has still room for improvement both in accuracy (sensitivity and specificity) and in the time before birth where hypoxia is detected.

NCD technique was successfully used for clustering the fetuses of a multicentric study with the aim of identifying the abnormal ones [17].

It is remarkable that, using sliding windows and NCD, both frequency indices and moments obtain the best accuracies in the 4 ↔ 3 hours interval whereas time indices obtain the best results in the 3 ↔ 2 hours interval. Our comparisons show that the commonly used Time and Frequency indices can be complemented by the moments, which are always applicable and do not suffer from signal losses. In addition, fetus movement might provide

valuable information as we noted when analyzing raw signals (Table 1), and when we observed the performance of $P_{LF}/(P_{MF} + P_{HF})$ index, which depends on fetus movement (Table 4). Finally, by adding similarity matrices selected by FS a promising 0.88 accuracy is reached in the $4 \leftrightarrow 1$ hours interval, which compares entire records and mimics the processing of a fetus during labor.

Practical implementation of this approach as an plugin of the available CTG systems is straightforward. We recommend to perform a careful selection and labeling of FHR records. Then, the number of cases in the knowledge database and processing capabilities must be balanced. For instance, the analysis of an FHR record every minute against a knowledge database of 1000 patients is easily done in a normal PC using gzip as compressor.

The decision making during the labor is a difficult task for the gynecologist. It always should be intended to be as less invasive as possible, but, of course, ensuring fetal well-being and acting as soon as possible in case of suspicion of fetal hypoxia. Our main contribution shows how the NCD analysis of the readily available FHR traces may help the gynecologists to make the correct decisions. We reach 88% accuracy, which is a remarkable result if we take into account that we are actually identifying stressed fetuses 3 hours before delivery that were not detected by the gynecologist until a later stage. This general methodology is also applicable to other time series classification problems and it is both simple to understand and simple to apply.

The results obtained in this study indicate that a further study with more patients should be performed to open the application of this type of FHR analysis of the fetus condition to the industry.

Acknowledgements

The author Óscar Barquero Pérez has the support of a FPU Grant (AP2009-1726) from the Ministerio de Educación, Spanish Government. Authors want to thanks professor Antonio García Marques for his suggestions and thoughtful comments on LASSO models.

References

- [1] Cilibrasi R, Cruz AL, de Rooij S, Keijzer M. CompLearn. <http://www.complearn.org>, 2008.
- [2] Signorini MG, Magenes G, Cerutti S, Arduini D. Linear and nonlinear parameters for the analysis of fetal heart rate signal from cardiotocographic recordings. *IEEE Trans Biomed Eng* March 2003;50(3):365–74. ISSN 0018-9294.
- [3] van Laar JOEH, Peters CHL, Vullings R, Houterman S, Oei SG. Power spectrum analysis of fetal heart rate variability at near term and post term gestation during active sleep and quiet sleep. *Early Hum Dev* December 2009;85(12):795–8. ISSN 1872-6232.
- [4] Pincus SM. Approximate entropy as a measure of system complexity. *Proc Natl Acad Sci USA* March 1991; 88(6):2297–301. ISSN 0027-8424.
- [5] Richman JS, Moorman JR. Physiological time-series analysis using approximate entropy and sample entropy. *Am J Physiol Hear Circ Physiol* June 2000;278(6):H2039–2049.
- [6] Ayres-de Campos D, Bernardes Ja. Twenty-five years after the FIGO guidelines for the use of fetal monitoring: time for a simplified approach? *Int J Gynaecol Obstet* July 2010; 110(1):1–6. ISSN 1879-3479.
- [7] Rajendra Acharya U, Paul Joseph K, Kannathal N, Lim CM, Suri JS. Heart rate variability: a review. *Med Biol Eng Comput* December 2006;44(12):1031–51. ISSN 0140-0118.
- [8] Goldberger AL, West BJ. Fractals in physiology and medicine. *Yale J Biol Med* 1987;60(5):421–35. ISSN 0044-0086.
- [9] Amer-Wahlin I, Hellsten C, Noren H, Hagberg H, Herbst A, Kjellmer I, Lilja H, Lindoff C, Mansson M, Martensson L. Cardiotocography only versus cardiotocography plus ST analysis of fetal electrocardiogram for intrapartum fetal monitoring: a Swedish randomised controlled trial. *Lancet* August 2001;358(9281):534–538. ISSN 01406736.
- [10] Ayres-de Campos D, Ugwumadu A, Banfield P, Lynch P, Amin P, Horwell D, Costa A, Santos C, Bernardes Ja, Rosen K. A randomised clinical trial of intrapartum fetal monitoring with computer analysis and alerts versus previously available monitoring. *BMC Pregnancy Childbirth* January 2010;10:71. ISSN 1471-2393.
- [11] Warrick PA, Hamilton EF, Precup D, Kearney RE. Classification of normal and hypoxic fetuses from systems modeling of intrapartum cardiotocography. *IEEE Trans Biomed Eng* April 2010;57(4):771–9. ISSN 1558-2531.
- [12] Dong S, Boashash B, Azemi G, Lingwood BE, Colditz PB. Automated detection of perinatal hypoxia using time-frequency-based heart rate variability features. *Med Biol Eng Comput* February 2014;52(2):183–91. ISSN 1741-0444.
- [13] Yang YX, Xie BS, Zhou ZX, Liu JN, Xue YY, Lv GL. Computer analysis system of blood oxygen saturation in an animal hypoxia model. *Med Biol Eng Comput* May 1998; 36(3):355–358. ISSN 0140-0118.
- [14] Siristatidis C, Salamalekis E, Kassanos D, Loghis C, Creatas G. Evaluation of fetal intrapartum hypoxia by middle cerebral and umbilical artery Doppler velocimetry with simultaneous cardiotocography and pulse oximetry. *Arch Gynecol Obstet* December 2004;270(4):265–70. ISSN 0932-0067.
- [15] Mori A, Iwashita M, Takeda Y. Haemodynamic changes in IUGR fetus with chronic hypoxia evaluated by fetal heart-rate monitoring and Doppler measurement of blood flow velocity. *Med Biol Eng Comput* May 2014;51(S1):S49–S58. ISSN 0140-0118.
- [16] Tichauer KM, Wong DYL, Hadway JA, Rylett RJ, Lee TY, St Lawrence K. Assessing the severity of perinatal hypoxia-ischemia in piglets using near-infrared spectroscopy to measure the cerebral metabolic rate of oxygen. *Pediatr Res* March 2009;65(3):301–6. ISSN 1530-0447.

- [17] Costa Santos C, Bernardes J, Vitanyi PMB, Antunes L. Clustering Fetal Heart Rate Tracings by Compression. In Comput. Med. Syst. 2006. CBMS 2006. 19th IEEE Int. Symp. ISSN 1063-7125, 2006; 685–690.

Address for correspondence:

O Barquero-Pérez
Department of Signal Theory and Communications
University Rey Juan Carlos. B104, Camino del Molino s/n
28943 - Fuenlabrada (Madrid), Spain
Phone: +34 91 488 84 62
oscar.barquero@urjc.es